Molecular Therapy
Nucleic Acids
Original Article

Improved loss-of-function CRISPR-Cas9 genome editing in human cells concomitant with inhibition of TGF-β signaling

Tarun Mishra,[1] Vipin Bhardwaj,[1] Neha Ahuja,[2] Pallavi Gadgil,[1,3] Pavitra Ramdas,[1] Sanjeev Shukla,[2] and Ajit Chande[1]

[1]Molecular Virology Laboratory, Department of Biological Sciences, Indian Institute of Science Education and Research (IISER) Bhopal, Bhopal 462066, India; [2]Epigenetics and RNA Processing Laboratory, Department of Biological Sciences, Indian Institute of Science Education and Research (IISER) Bhopal, Bhopal 462066, India

Strategies to modulate cellular DNA repair pathways hold immense potential to enhance the efficiency of CRISPR-Cas9 genome editing platform. In the absence of a repair template, CRISPR-Cas9-induced DNA double-strand breaks are repaired by the endogenous cellular DNA repair pathways to generate loss-of-function edits. Here, we describe a reporter-based assay for expeditious measurement of loss-of-function editing by CRISPR-Cas9. An unbiased chemical screen performed using this assay enabled the identification of small molecules that promote loss-of-function editing. Iterative rounds of screens reveal Repsox, a TGF-β signaling inhibitor, as a CRISPR-Cas9 editing efficiency enhancer. Repsox invariably increased CRISPR-Cas9 editing in a panel of commonly used cell lines in biomedical research and primary cells. Furthermore, Repsox-mediated editing enhancement in primary human CD4$^+$ T cells enabled the generation of HIV-1-resistant cells with high efficiency. This study demonstrates the potential of transiently targeting cellular pathways by small molecules to improve genome editing for research applications and is expected to benefit gene therapy efforts.

INTRODUCTION

CRISPR-Cas9 is at the forefront of genome editing technologies.[1,2] It has been widely exploited for research applications including epigenetic modifications,[3,4] tagging endogenous genes,[5,6] live imaging of genome editing and transcription,[7] and, most important, manipulating genes for therapeutic benefits.[8] The CRISPR-Cas9 genome editing platform uses Cas-gRNA (guide RNA) ribonucleoprotein (RNP) complex that generates a double-strand break (DSB) in the target sequence. Following the DSB, cellular DNA damage repair response recruits various factors to repair the incised DNA strands either by classical/alternative NHEJ (non-homologous end-joining) or by HDR (homology-directed repair).[9–11] Donor template availability is a constraint for HDR. In the absence of a donor, NHEJ-mediated repair results in the deletion of or disruptions in the target sequence. Thus, NHEJ-mediated repair is one of the most commonly used methods for generating loss-of-function edits by CRISPR-Cas9.

Although CRISPR-Cas9 holds the ability to manipulate the genome in a relatively simplistic manner, achieving greater efficiency in human cells, especially in primary cells, remains a universal concern. This is likely due to repressive mechanisms or competing signals that counter the CRISPR-Cas9 function. Therefore, we posited that small-molecule targeting of potential competing mechanisms would help obtain the edits with improved efficiency in human cells.

In this study, we describe a reporter assay to screen small molecules for improved loss-of-function editing. A large-scale chemical screen performed using this reporter assay identified Repsox as an enhancer of CRISPR-Cas9-based loss-of-function editing. Repsox inhibits the binding of ATP to TGF-βRI/ALK5, thereby inhibiting TGF-β signaling and SMAD2/3 phosphorylation.[12,13] TGF-β signaling is associated with cellular processes such as embryonic development, cell proliferation, immunomodulation, and others.[14] More recently, TGF-β signaling has been linked to DNA damage response; as shown by Kim et al.,[15] TGF-β signaling activates DNA LIG4, a crucial factor of the classical NHEJ DNA repair pathway. On the other hand, TGF-β signaling also inhibits BRCA1, ATM, and MSH2, which are critical factors for the repair of DSB induced by ionizing radiation. Interestingly, human papilloma virus (HPV) infection phenocopies the effect of TGF-β signaling inhibition[16] similar to that seen in cells treated with inhibitors of TGF-β receptor.

Here we demonstrate that treatment of cells of different tissue origins with Repsox improves loss-of-function editing, regardless of the mode of Cas9 and guide RNA expression. Finally, we provide a proof of concept using clinically relevant cells to expand the utility of Repsox as a CRISPR-Cas9 editing enhancer for potential gene therapy applications.

Received 24 July 2021; accepted 3 March 2022;
https://doi.org/10.1016/j.omtn.2022.03.003.

[3]Present address: Department of Biology, Indiana University, Bloomington, IN 47405, USA

Correspondence: Ajit Chande, Department of Biological Sciences, Indian Institute of Science Education and Research (IISER), Academic Building-3, Bhopal By-pass Road, Bhauri, Bhopal, Madhya Pradesh 462066, India.
E-mail: ajitg@iiserb.ac.in

RESULTS

A high-throughput reporter assay for loss-of-function CRISPR screen

Being a stable, convenient, and sensitive visual reporter, GFP is one of the most preferred targets for genome editing assay readout in high-throughput screens. However, its intracellular accumulation due to a longer half-life (~26 h)[17] poses problems in assays that detect loss of GFP function. Therefore, a less stable form of GFP is desirable for high-throughput loss-of-function CRISPR screens. Previously researchers have developed an unstable GFP by tagging it with a Tsp protease recognition sequence that reduced its half-life for understanding the cellular process in prokaryotic systems.[18,19] In mammalian cells, programmed proteolysis allows rapid destruction of cyclins to regulate the cell cycle. This is facilitated by the cyclin destruction box (CDB) sequence.[17,20] Because of the ability of CDB to render a protein for degradation, we fused CDB at the N terminus of the GFP sequence for expeditious estimation of GFP loss as a function of editing. A rapid clearance concomitant with less fluorescence accumulation was detected for the modified GFP fused with CDB (mGFP) (Figure 1A). A time course analysis in parallel with unmodified GFP revealed that mGFP′ half-life was reduced to 6–10 h (Figure S1A), enabling rapid measurement of genome editing efficiency.

Using the mGFP reporter, we devised a chemical screen to discover small-molecule modulators on the basis of their ability to enhance loss-of-function editing. A variant of SpCas9 referred to as eSpCas9 (hereafter referred to as Cas9) was used because of its relatively higher fidelity.[21] The cells were transfected in different sets with indicated plasmids to measure the loss of GFP fluorescence as a function of CRISPR-Cas9 editing without affecting the RFP (internal control) signal (Figure 1B). To further confirm that the loss of mGFP fluorescence is because of indels in the mGFP encoding sequence, we amplified the target locus using PCR. Sanger sequencing of the PCR product followed by TIDE analysis showed 36% editing in these experimental settings, thus providing room for further improvement (Figure S1B).

Using these optimized conditions, we performed an unbiased chemical screen (3,072 treatment conditions in total) to identify those that promote loss of function phenotype (Figure 1C). We randomly selected three plates to check the robustness of the assay that consistently yielded an average Z′ of 0.815 (Figure 1D). The library used in the screen comprises 1,280 biologically active small molecules targeting receptors, ion channels, kinases, and so forth, involved in various biological processes (Figure 1E). Ratiometric analysis (RFP/GFP) enabled the identification of small molecules that promoted loss of mGFP fluorescence as a function of CRISPR-Cas9 editing (Figure 1F). Next, hit selection was carried out by setting the cut-off of $\geq$1.5-fold increment by small molecules compared with editing with the DMSO control. Eighty-two compounds qualified this hit selection criterion from the primary screen and were selected further for the secondary screen, which yielded an average Z′ of 0.727 (Figures 1G and 1H).

Repsox promotes loss-of-function editing

A secondary screen identified Repsox as one of the prominent candidates that increased editing efficiency by six-fold at 10 μM concentration without much effect on cell viability (Figure 2A). In contrast, IOX2, a compound that displayed the highest RFP/GFP ratio (Figure 1G), exhibited ~50% cell death at 10 μM (Figure S2A), thus barring us from using it for subsequent characterization. Repsox showed maximum effect (14-fold editing enhancement) at 50 μM concentration. However, the cellular growth monitored at various concentrations indicated that Repsox is well tolerated at 10 μM concentration, with 6-fold enhancement in the editing efficiency in these experimental conditions (Figures 2A and 2B). We also edited the *GFP* locus in HT1080 and A549 cells using variable concentrations of Repsox (Figure S2B and S2C). In parallel, the cell viability of HT1080 and A549 cells was examined using Alamar Blue assay (Figure S2D and S2E). By observing the GFP editing efficiency and cell viability from three cell lines, we found that Repsox can promote gene editing at 5–10 μM concentration without apparent adverse effects on target cells.

Next, we interrogated whether the effect of Repsox is transfection dependent. To this end, we integrated the target locus (mGFP cassette) by lentiviral transduction in a T cell line (Jurkat). In parallel, the locus was also lentivirally integrated into the genome of HEK293T. The treatment of Repsox induced a 2.43-fold increase of locus editing efficiency in HEK293T and 3.26-fold in Jurkat T cells (Figures 2C and 2D). We also examined whether this was a lot- or manufacturer-specific effect. The compound obtained from two different manufacturers yielded comparable results and performed equally well in the assay conditions (Figure S3A). Additional experiments to characterize the compound using mass spectrometry further confirmed its identity (Figure S3B).

AZT, another small molecule known to enhance CRISPR-Cas9 editing,[22] was used at the concentration reported earlier to compare its efficiency with Repsox. We observed loss of GFP in lentivirally transduced HEK293T and A549 cells for both AZT and Repsox treatment conditions. Whereas AZT increased 2.01- and 2.6-fold editing in HEK293T and A549 cells, respectively, Repsox enhanced GFP editing by 2.8- and 3.13-fold (Figure S4A and S4B).

To explore the editing-enhancement potential of Repsox on genes other than GFP, we generated stable firefly luciferase-expressing cell lines (HeLa, A549, HT1080, HEK293T, K562, and JTAg) using lentiviral transduction. Loss of a functional CDS by indels was expected to produce reduced luminescence in these engineered cells (Figure S5). Editing the luciferase locus also reproduced the Repsox effect in stimulating genome editing in these cells of different tissue origins (Figure 2E). Representative luciferase units from individual cell lines indicated a consistent enhancement of editing by Repsox that ranged from 1.5- to 4-fold. Furthermore, to exclude the possibility if Repsox decreases the expression of GFP and firefly luciferase independently of Cas9 and guide RNA, cells stably expressing luciferase or GFP were grown with either vehicle or

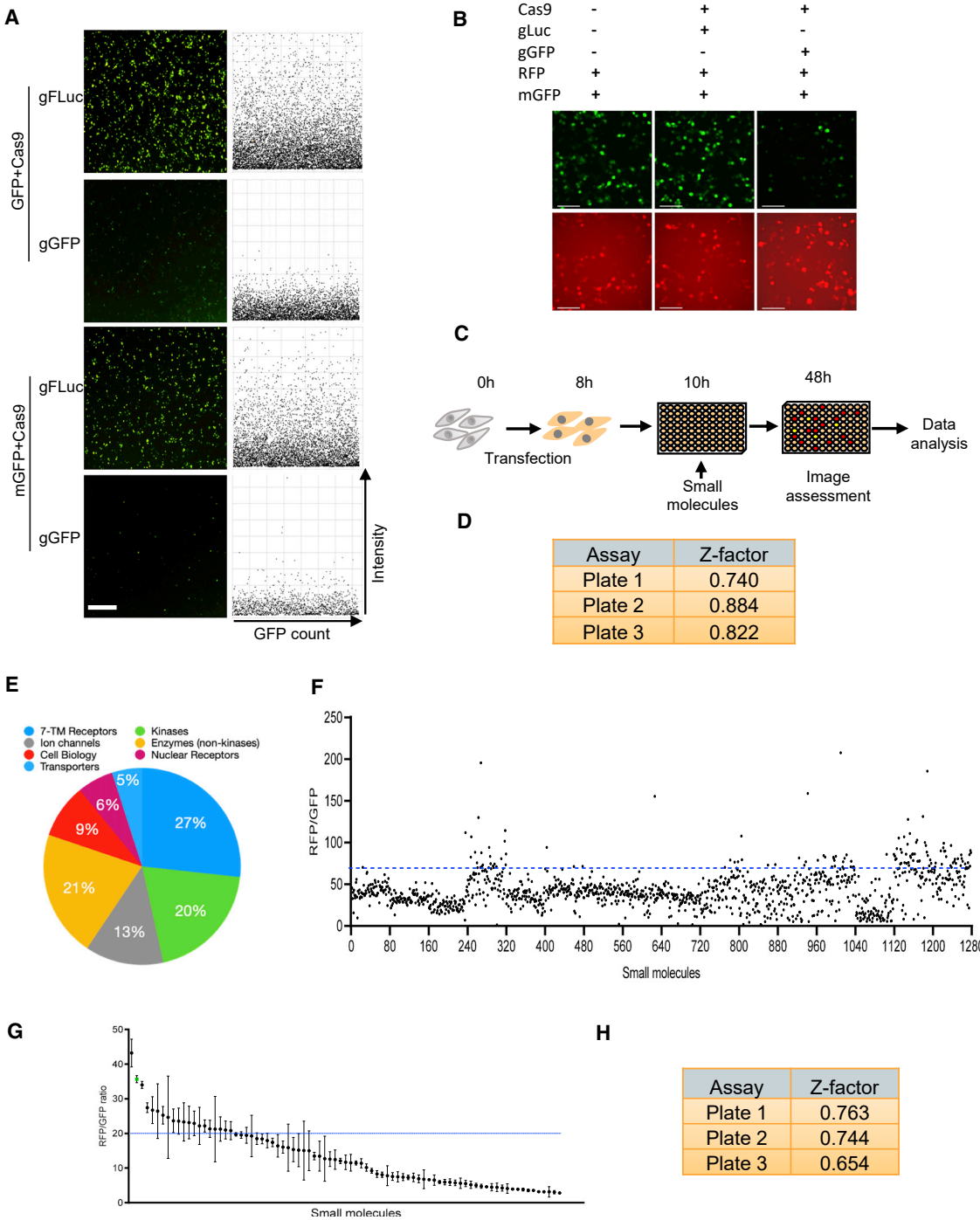

Figure 1. A rapid screening assay to identify loss-of-function editing enhancers

(A) Rapid loss of mGFP compared with GFP by CRISPR-Cas9 editing as shown in representative images (scale bar, 200 μm) and corresponding intensity plots. (B) Representative images of a screen-ready assay indicating an internal RFP reporter (scale bar, 100 μm). (C) Schematics of the chemical screen setup and the robustness evaluated from three randomly selected plates (D). (E) Classes of small molecules used in the screen. (F) A scatterplot depicting a primary screen produced by plotting an RFP/GFP ratio with a cut-off line. (G) Secondary validation screen (n = 3, ±SD) and hit selection (green dot indicates Repsox) on the basis of the robustness of the assay as obtained from three plates (H).

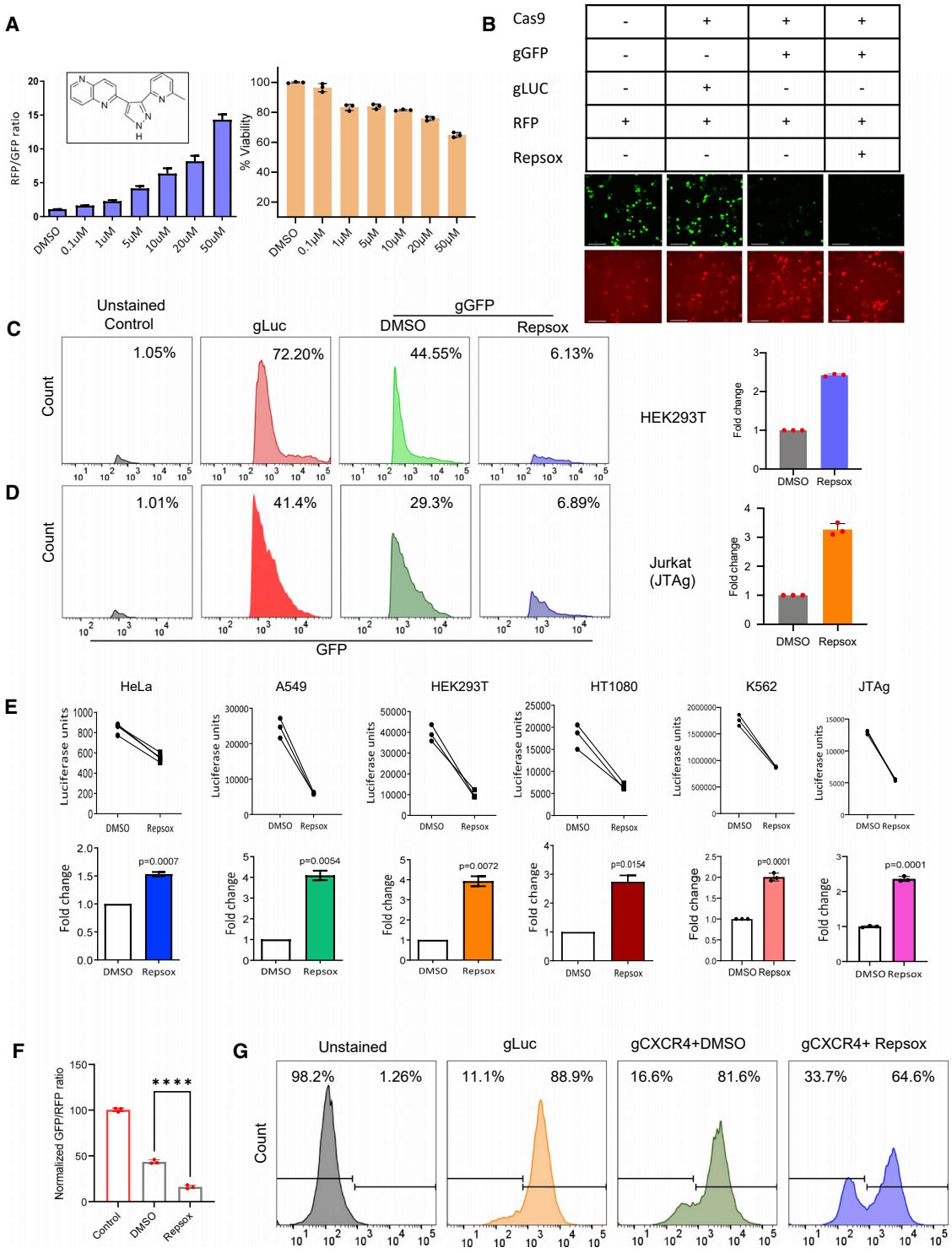

Figure 2. Repsox promotes loss-of-function editing

(A) Dose-dependent effects of Repsox on the loss of GFP, indicated by RFP/GFP ratio, in HEK293T cells transfected with gGFP, Cas9, GFP, and RFP and the structure of Repsox in the inset (left panel). Alamar blue assay to measure cell growth for corresponding concentrations of the Repsox (right panel); (n = 3, ±SD). (B) Representative images for mGFP editing at 10 μM concentration of the Repsox (scale bar, 100 μm). (C) The effect of the Repsox challenge on gene editing assessed using flow cytometry

(legend continued on next page)

Repsox (10 μM) for 48 h. Measurement of luciferase activity and GFP counts showed no reduction, discounting the possibility that Repsox directly affected these targets (Figure S6A and S6B).

We also examined the effects of Repsox treatment on global cellular transcriptome by collecting and analyzing the existing transcriptomics data (SRR12248355, SRR12248357, SRR12248367, and SRR12248369) of DMSO/Repsox-treated adenocarcinoma cells (SW480). Our analysis indicated minimal perturbations in the transcriptome upon Repsox treatment (Figure S6C). However, gene-editing enhancement was consistently observed for both GFP and luciferase genes in SW480 cells upon treatment with Repsox, thus indicating that Repsox plausibly affects signaling at protein level (Figure S6D and S6E). Furthermore, with two guide RNAs simultaneously targeting GFP, we found consistent editing enhancement by Repsox (Figure 2F).

The application of Repsox in promoting CRISPR-Cas9 editing for the endogenous loci (*CXCR4* and *SERINC5*) was investigated next. *CXCR4* editing was performed in cells of distinct tissue origins with the varying transcriptional status of the gene: HEK293T (kidney), K562 (bone marrow), and Jurkat (T cells). Reliably, the editing assays revealed that with Repsox treatment, there were 3.3-fold, 2.9-fold, and 2.13-fold enhancements in editing efficiency in HEK293T, K562, and JTAg (Jurkat) cells at the genomic level, respectively (Figure S7). T cells express *CXCR4*; hence we checked the editing efficiency for JTAg cells by immunostaining the CXCR4 protein. To avoid transfection-associated variability, electroporated JTAg cells were split into different wells that received either DMSO or Repsox. Consistently, the surface expression of CXCR4 analyzed using flow cytometry in JTAg suggested editing-associated loss of the endogenous CXCR4 in these cells (Figure 2G), measured at 3.32-fold higher when these cells received Repsox. Next, we checked the effect of Repsox on the editing of *SERINC5* locus.[23] For this, HEK293T, A549, and JTAg cells were transfected with Cas9 and gRNA specific to *SERINC5* and were split before treatment with either DMSO or Repsox for the next 48 h. The editing of the *SERINC5* locus in HEK293T, A549, and JTAg cells yielded 2.49-, 2.23-, and 1.79-fold enhancement with Repsox, respectively (Figure S8).

Repsox promotes on-target editing without affecting the cell cycle profiles and genome integrity

Given the potential risk for designer nuclease-associated off-target activity, we interrogated if Repsox treatment also promotes off-targeting of Cas9, in addition to enhancement of on-target editing. Using an online tool (http://crispr.mit.edu), we shortlisted *MAMLD1*, *SCARB1*, *AKT2*, and *ESRRG* genes. Cas9 could potentially target those, and the presence of Repsox was envisaged to introduce a manifold increase of off-targeting.[24] To examine this, the PCR-amplified products that represented a total pool of Repsox-treated cells were subjected to Sanger sequencing to find potential off-targeting due to the editing-enhancing effects of Repsox. TIDE analysis of off-target loci revealed that although gRNA introduced several indels in the *CXCR4* genomic locus, the putative off-target loci were not claimed to generate indels (Figure S9). In addition, we performed deep sequencing of all four loci (*MAMLD1*, *SCARB1*, *AKT2*, and *ESRRG*) from Repsox-treated *CXCR4*-edited HEK293T and JTAg cells. The analysis revealed insignificant editing ($\leq$0.5%) at *MAMLD1*, *SCARB1*, *AKT2*, and *ESRRG* loci in JTAg cells, compared with ~72% on-target editing. For HEK293T, we found 0.3%–0.8% editing at *MAMLD1*, *SCARB1*, *AKT2*, and *ESRRG* loci in HEK293T cells, respectively, with ~42% on-target editing (Figure 3). A spike seen for the *MAMLD1* target in the mutation position distribution plot was associated with an error in the oligo sequence. Altogether, the experiments indicated that the editing-enhancing effect of Repsox is on target, independent of the transcriptional status of the gene and not cell type specific.

After establishing on-target specificity, we asked if Repsox promotes the editing by arresting cells in a particular cell cycle phase. As G1 phase was known to increase the NHEJ-dependent repair,[25] the Repsox effect might have been coupled to its ability to arrest the cells in G1 phase. To test this, we determined the impact of Repsox on the cell cycle by EdU incorporation assay. It was observed that Repsox has an indiscernible effect on the profiles of HEK293T, JTAg, and K562 (Figure 4A). We also examined if Repsox alters genome stability and improves CRISPR-Cas9 editing. To this end, we performed a neutral comet assay[26] by challenging cells with DMSO, Repsox, or doxorubicin (a positive control). The length of the comet tail (Figure 4B, top panel) served as the measure of genome instability. It was observed that Repsox had an insignificant effect on inducing genome instability compared with doxorubicin, which showed a higher impact (Figure 4B, lower panel).

Repsox orchestrates editing enhancement via TGF-βRI inhibition

Repsox is reported to inhibit TGF-βRI and thereby downstream signaling.[12] TGF-βRI activates SMAD2/3 proteins, which, along with SMAD4, translocate to the nucleus and control the expression of genes having SMAD-response elements. We examined if the enhancement of genome editing efficiency correlates with the ability of Repsox to inhibit TGF-βRI-mediated signaling in the responsive MCF7 target cells functionally.[27] Accordingly, we confirmed the ability of Repsox to promote loss-of-function editing in MCF7 cells. The promotion of editing by Repsox (3.5-fold) (Figures 5A and 5B) was in agreement with the data obtained from a panel of cell lines of different tissue origins we tested in Figure 2. To validate further if editing enhancement was correlating with the ability of Repsox to suppress signaling downstream of TGF-βRI functionally, we used a luciferase reporter regulated by a downstream effector of TGF-βRI

(representative histogram panels) and the corresponding fold enhancement (right panel; n = 3, ±SD) from the lentivirally integrated mGFP cassette in the HEK293T cells (C) and Jurkat cells (D). Editing of engineered luciferase locus obtained by lentiviral integration into cell lines of various tissue origins as indicated (E). The lower panel shows fold enhancement of editing for corresponding cell lines (n = 3, ±SD). (F) Comparison of GFP editing using two guide RNAs simultaneously targeting the GFP locus (n = 3, ±SD). (G) Representative flow cytometry histograms of JTAg cells stained for CXCR4 under various indicated treatment conditions.

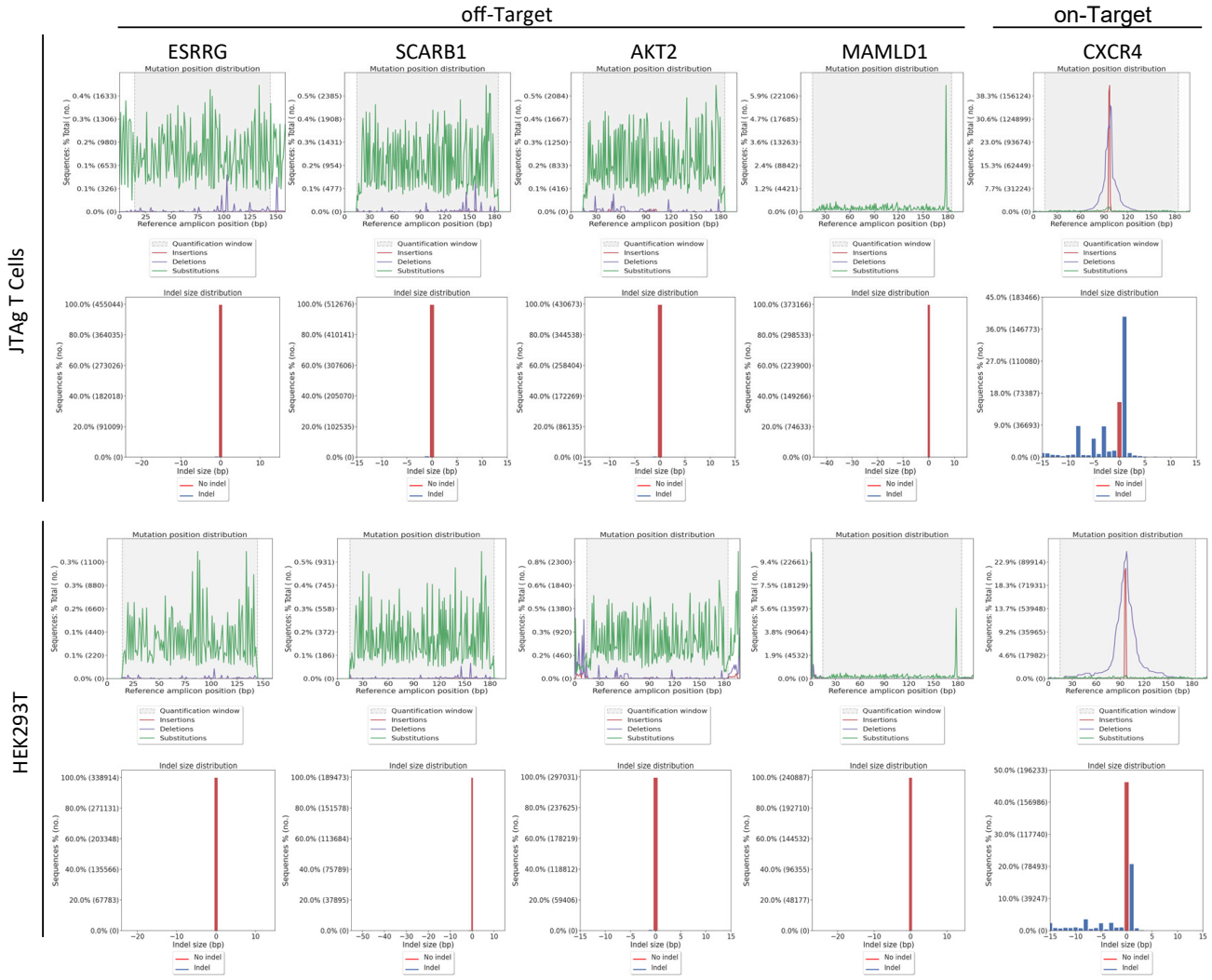

Figure 3. Targeted deep sequencing analysis

Editing percentage in Repsox-treated JTAg and HEK293T cells expressed as sequence percentage of total reads. Next-generation sequencing (NGS) was performed for five loci (one on-target and four off-targets [*ESRRG*, *SCARB1*, *AKT2,* and *MAMLD1*]).

(SMAD). Although Repsox inhibited transcriptional induction of luciferase gene from a reporter plasmid by suppressing TGF-βRI-dependent SMAD activation, the on-target genome editing enhancement was explicitly observed with gRNA specific to the GFP in MCF7 cells (Figure 5C). We see that the effect of Repsox on TGF-βRI targeting is not influenced by the gRNA, as a non-targeting gRNA allowed the suppression of luciferase induction from SMAD RE but did not edit the GFP encoding sequence (Figure 5C). We also confirmed whether enhanced editing efficiency of Repsox is because of the increased expression or stabilization of Cas9. Western blotting from the Cas9 expressing cells, however, indicated no significant differences in expression of Cas9 (Figure 5D).

Having confirmed the ability of Repsox to target the TGF-βRI in the target cells, we next asked if the removal of this upstream factor would phenocopy the effects of Repsox. Accordingly, we generated HEK293T and HeLa TGF-βRI-knockout cells (Figure 5E) and checked the extent of editing due to the loss of TGF-βRI in these cells. The results indeed suggested that loss of TGF-βRI is sufficient to phenocopy the effects observed with Repsox treatment (Figures 5F–5I) and that the loss of TGF-βRI can make cells insensitive to enhancing effects of Repsox on genome editing (Figures 5G and 5I). Altogether, these results using transfection and virus transduction assays demonstrated that the activity of Repsox in promoting loss-of-function genome editing is TGF-βRI dependent.

Next, we asked how long the Repsox treatment sustains its effect in cells. For this, we transfected HEK293T cells with SMAD reporter and Renilla luciferase-expressing plasmids (transfection control).

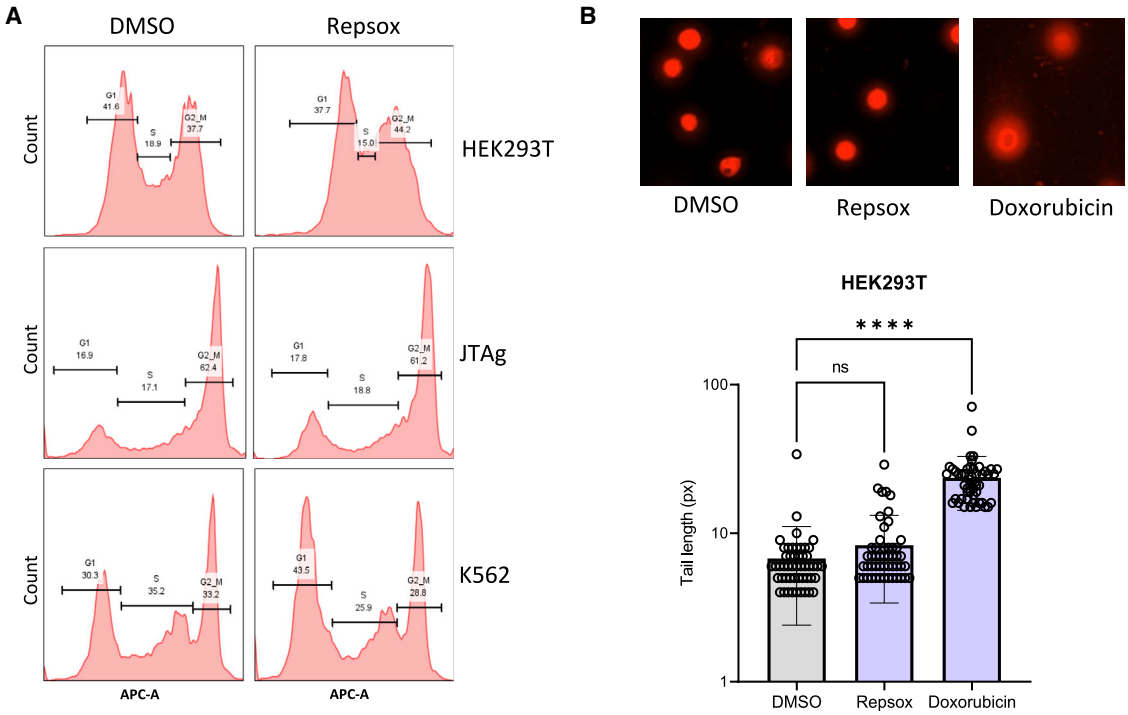

Figure 4. Effects of Repsox on cell cycle and genome integrity

(A) Flow cytometry profiles of HEK293T, Jurkat TAg (JTAg), and K562 cells treated either with DMSO or Repsox (10 μM) for 48 h and observed for cell cycle phases. (B) Representative images of comets in the indicated conditions (upper panel). Graph representing the length of DNA tail observed from HEK293T cells when treated with DMSO, Repsox (10 μM), and doxorubicin (20 μM) (lower panel) (n = 50, ±SD). *p < 0.05, **p < 0.01, ***p < 0.001, and ****p < 0.0001; ns, nonsignificant.

Subsequently, transfected cells were treated with Repsox (10 μM), and SMAD reporter kinetics were assessed in the indicated conditions. Luciferase activity from the SMAD reporter showed a gradual decrease in the SMAD-dependent luciferase expression, reaching close to background at 72 h after the addition of Repsox. Furthermore, to assess whether Repsox-treated cells regained TGF-β signaling competence, we removed Repsox after 48 h and incubated the cells for an additional 24 h before the luciferase activity was measured. Results from these experiments showed complete recovery of luciferase expression after 96 h of Repsox removal from the cell culture medium (Figure S10).

Virus-like particles enable Cas9 RNP delivery

Integrating lentiviral vectors offer advantages of efficiency and are extensively used to express CRISPR-Cas9 components persistently. However, the risk for genomic insertions and persistent expression of the Cas9 endonuclease may be undesirable and may provoke unintended genomic alterations. Accordingly, a traceless delivery of gRNA complexed Cas9 would be ideal as a "hit-and-go" approach (Figure 6A). Coupled with small-molecule enhancers of genome editing, it would prove an effective gene-editing platform. Therefore, we sought to develop a Cas9-packaging strategy for a traceless delivery of CRISPR components into human cells. We recognized that the U6 promoter renders the expression of gRNAs in the nucleus and would impair packaging into budding Cas9 virus-like particles (VLPs). To circumvent this, we expressed the gRNAs from a human glutamine tRNA promoter for cytoplasmic expression of guides. This modification enabled the generation of VLPs that efficiently packaged Cas9 (Figure 6B). The transient expression of Cas9 protein is expected to reduce the off-target activity associated with prolonged expression. To confirm, the Cas9 intracellular levels from Cas9-VLP-treated cells and cells expressing nuclease from a transfected plasmid were compared next. Cas9 from the VLPs was detectable after 4 h of transduction in target cells, and the signal disappeared by 24 h. On the contrary, the Cas9 expressed from the transfected plasmid was detected after 8 h of transfection and subsequently accumulated in the cells (Figure 6C). The packaging of Cas9 RNPs in VLPs permitted editing of the desired locus in target cells, albeit with low efficiency. The Repsox challenge, however, promoted the editing efficiency of Cas9 VLPs in a locus and cell line-independent manner (Figures 6D–6F). We next checked the ability of Cas9-VLPs to edit the endogenous *CXCR4* locus in the human primary T cells and found that VLPs can deliver Cas9 components and that the Repsox challenge improves genome editing efficiency in primary cells. Editing of *CXCR4* gene by Cas9 VLPs in primary cells showed a 1.74-fold increase when treated with Repsox compared with DMSO (Figure 6G). Altogether these experiments confirmed the presence of inhibitory mechanisms in the cells that dampen the CRISPR-Cas9 loss-of-function editing efficiency regardless of

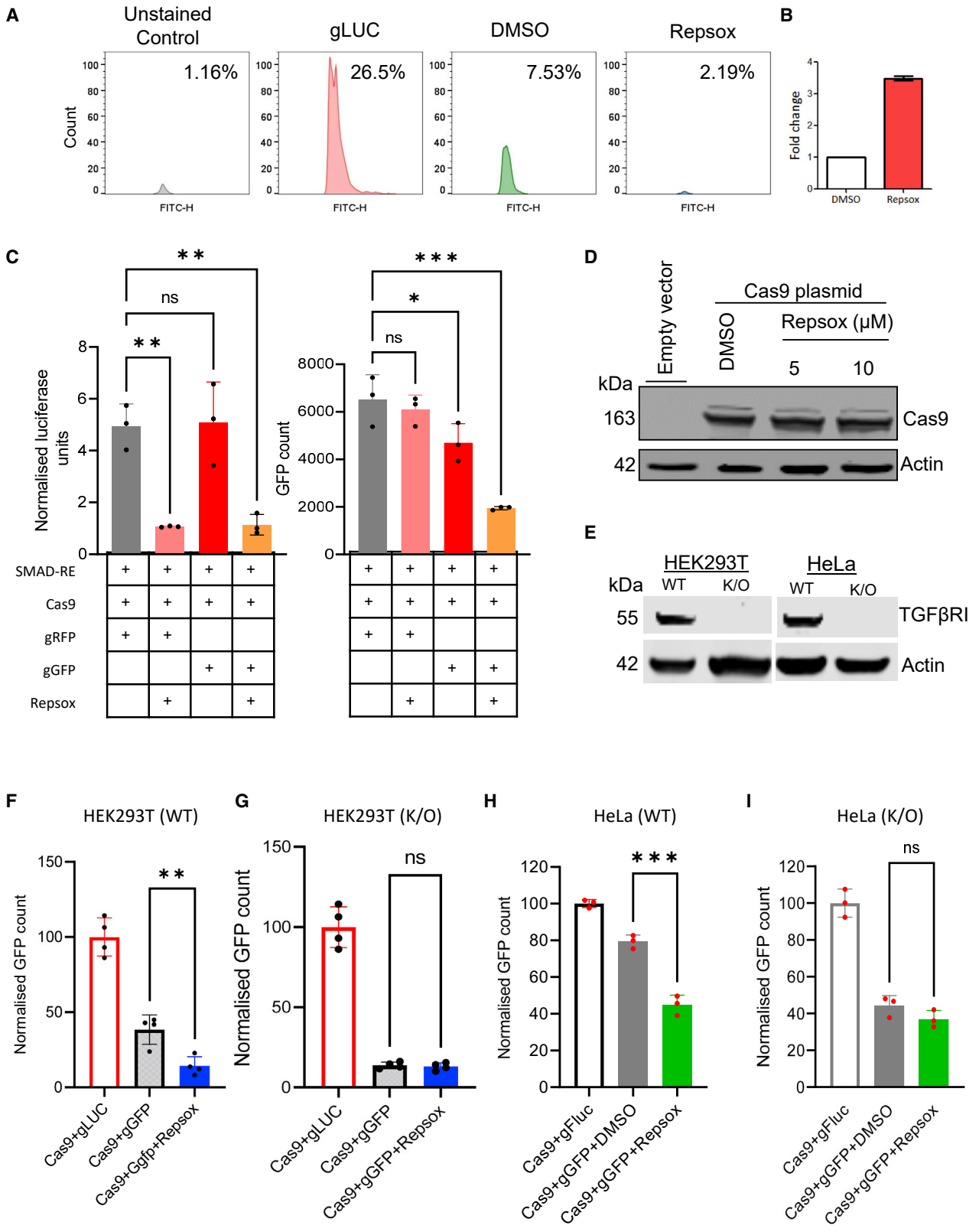

(legend on next page)

the cell type and mode of expression of CRISPR components and that Repsox relieves this block.

Repsox-augmented editing enables the generation of HIV-1-resistant T cells

Controlling the DNA repair pathway choice for the desired outcome without affecting the viability of clinically relevant cells would prove beneficial for therapeutic genome editing. If achieved, it can be used effectively for *ex vivo* gene or cell therapy. CRISPR-Cas9 offers unprecedented avenues for *ex vivo* manipulation of defective genes in hematopoietic lineages for treatment of blood disorders or generating the cells that resist infection from viruses such as HIV-1. Forty years after the first description of HIV/AIDS, the disease remains incurable, and improved therapeutic approaches are clearly required for achieving a functional cure. Therefore, we next investigated if Repsox exhibited similar effects in primary cells to those observed with various human cell lines. We selected primary T cells as a model because of their widespread use in gene/cell therapy for infection and cancer. As a proof of concept, we targeted HIV co-receptor CXCR4 in the $CD3^+/CD4^+$ primary T cells isolated from healthy donors and enriched to purity (Figure S11). The CXCR4 gRNA-transduced cells were challenged with DMSO or Repsox to check the effect on CXCR4 expression in primary $CD4^+$ T cells post-editing. Without much of an impact on cell viability (Figure S12), we observed 1.65- to 3.31-fold enhancement, irrespective of the donor background (Figure 7). These experiments suggest that the effect of Repsox on genome editing enhancement is consistent in primary cells. We next asked if the enhanced editing of the *CXCR4* locus in the primary $CD4^+$ cells by Repsox would make them relatively more refractory to X4-tropic HIV-1 infection. Indeed, Repsox treatment made the edited primary CD4 cells 2.14- to 3.07-fold more resistant to X4-tropic HIV-1 than DMSO-treated counterpart (Figure 8). Altogether these experiments suggested the applicability of this approach in generating an HIV-resistant pool of primary human $CD4^+$ cells efficiently for potential clinical and research applications.

DISCUSSION

Many organisms naturally experience DSBs. However, unintended DSBs caused by endogenous and exogenous factors are potentially lethal to the cell. If unrepaired, such breaks may potentially lead to physiological defects. Thus, DSBs must be prevented and repaired by the cells as they occur. Breaks such as those generated by CRISPR-Cas9 are no exception and are often resisted by various intrinsic cellular mechanisms that we have begun to appreciate.[28] Upon DNA DSBs, the HDR and NHEJ repair pathways compete with each other, and various upstream regulators modulate these pathways and the DNA repair outcomes. DNA repair by NHEJ is the most widely accepted approach for generating loss-of-function edits by CRISPR-Cas9 and has been of great interest to the research community.[29,30]

We demonstrated that biologically active small molecules, such as Repsox, can be repositioned for genome editing improvement by inhibiting competing signals that interfere with CRISPR-Cas9 functioning. Compared with genetic manipulations, small molecules have many advantages: ease of use, a higher degree of control, and effects that can be fine-tuned by varying their concentrations and combinations. The high efficiency, fast mode of action, reversibility, and easy application offer several advantages. Repsox has already been proved not to have any adverse effects on primary human cells.[12,31,32] The compound is available from various manufacturers, is specific, does not display undesired effects, and promotes on-target genome editing. Experimental designs that allow higher transfection efficiency/delivery of Cas9 RNP in conjunction with these compounds are expected to offer superior efficiency.

Furthermore, we confirmed the augmenting effects of Repsox by different gene transfer modalities: calcium phosphate co-precipitation, electroporation, lipoplexes, integrating lentiviruses, and delivery of Cas9-RNPs via VLPs. Although efficiencies associated with each of these methods reflected the expression levels of payload delivered and concomitant basal editing efficiencies, the Repsox effect remained conserved regardless. Delivery of CRISPR-Cas9 components perhaps remains the most significant bottleneck to genome editing. VLP delivery mode and treatment with small molecules such as those demonstrated in this report can reduce possible off-target mutations relative to other methods such as nucleic acid delivery by transfection, integrating viral vectors because of the short half-life of RNPs.[33,34]

Small molecule-mediated removal of the inhibitory cues appears to promote respective pathways triggering to repair the locus following DSBs generated by Cas9. Here we demonstrated that TGF-βRI-dependent signaling could modulate the efficiency of loss-of-function editing. Despite its ability to regulate critical factors involved in DNA repair, the role of TGF-β signaling in genome integrity remains poorly understood.[15,35–39] Recent reports have implicated TGF signaling inhibition as an adjunct for enhancing genotoxic sensitivities across cancer types,[39] suggesting an exciting parallel that, in principle, is applicable to loss-of-function CRISPR-Cas9 editing. Using complementary approaches, we established that Repsox promoted editing by inhibiting the upstream signaling orchestrated through the TGF-β receptor and that the genetic

Figure 5. Repsox orchestrates editing enhancement effect through TGF-β receptor

(A) MCF7 cells seeded in 24-well plate and transfected with mGFP along with Cas9, gGFP-expressing plasmids further treated with DMSO and 10 μM Repsox for 48 h and analyzed by FACS for residual GFP positivity. (B) Fold change in GFP expression from DMSO- and Repsox-treated experimental sets. (C) SMAD inhibition by Repsox (left) and increase in the editing of GFP plotted as luciferase units and GFP count, respectively (right) (n = 3, ±SD). (D) Cas9 protein expression by western blotting after treatment of Cas9 expressing HEK293T cells with DMSO or Repsox (5 and 10 μM). Actin served as a loading control. (E) Western blot depicting expression of TGF-βRI in wild-type (WT) and knockout (K/O) HEK293T and HeLa cells. Actin served as a loading control. Effect of TGF-βRI knockout on the genome editing enhancement and sensitivity to Repsox in (F and G) HEK293T (n = 4, ±SD) and (H and I) HeLa cells (n = 3, ±SD). *$p < 0.05$, **$p < 0.01$, ***$p < 0.001$, and ****$p < 0.0001$; ns, nonsignificant.

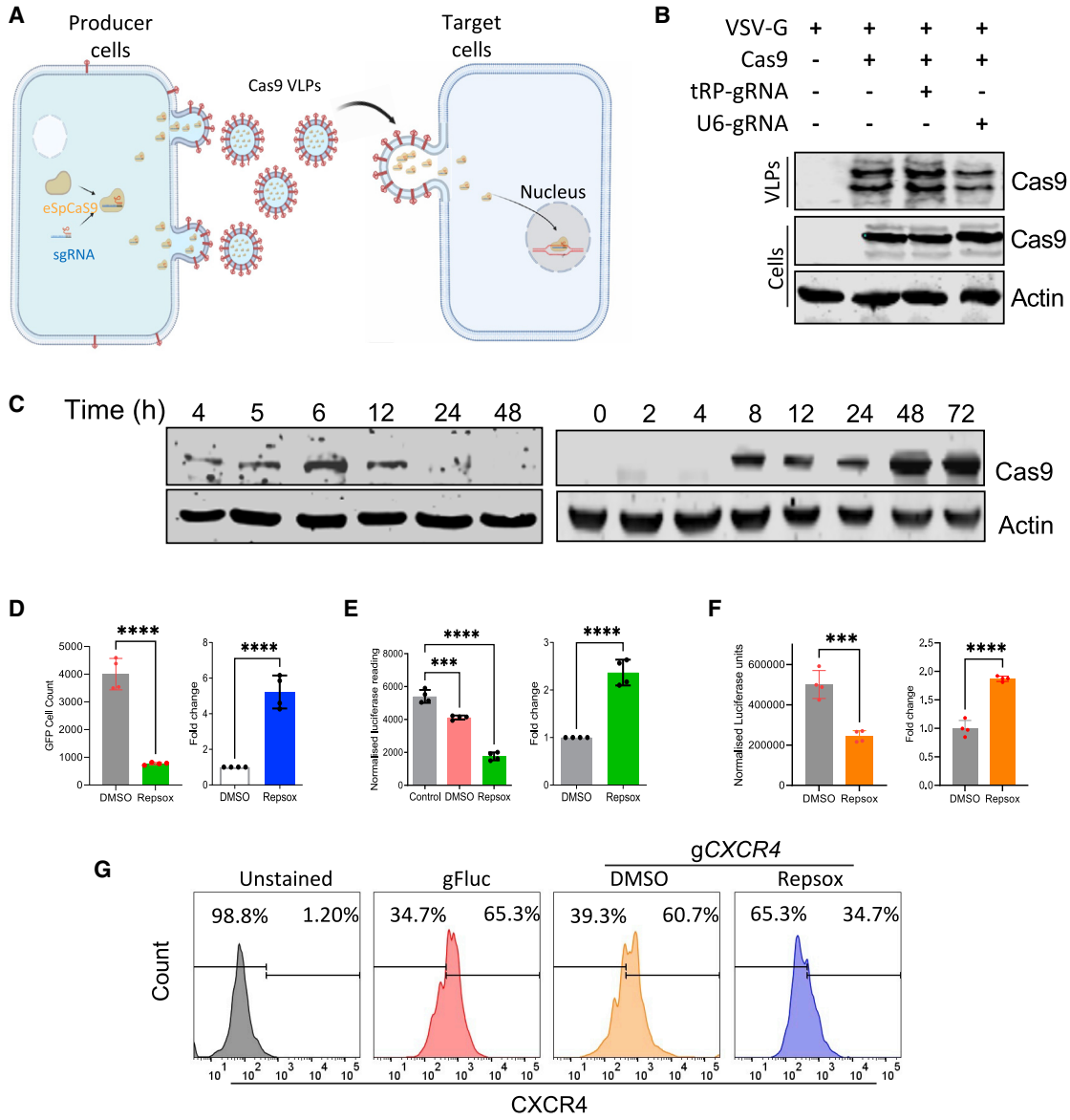

Figure 6. Cas9 VLP-mediated genome editing and enhancement by Repsox

(A) Schematics of Cas9 RNP complex packaging in VLPs and delivery to target cells. (B) Western blot of analysis of Cas9 from the producer cells and from VLP under indicated conditions. (C) Cas9 intracellular levels from Cas9-VLPs transduced (left) or Cas9-expressing plasmid transfected cells (right) at indicated time points. The reported time points correspond to the time of analysis following transduction or transfection. (D) Editing in HEK293T mGFP stable cells by Cas9 VLPs and fold increase in GFP-editing with Repsox. Luciferase editing in stable cell lines with Cas9 VLPs with a fold increase in editing using Repsox in (E) HEK293T (n = 4, ±SD) and (F) K562 (n = 4, ±SD). (G) Representative flow cytometry histograms depicting Repsox-mediated enhancement genome editing using Cas9 VLPs targeting CXCR4 in primary human CD4+ cells. *p < 0.05, **p < 0.01, ***p < 0.001, and ****p < 0.0001; ns, nonsignificant.

removal of this upstream factor makes the cell insensitive to the action of Repsox.

Given that an alternative repair process can occur in the absence of HDR and classical NHEJ, Repsox-promoted editing could be associated with an alternative repair mechanism. The TGF signaling appears to profoundly affect repair processes via the expression and molecular regulation of many genes.[38] It remains to be established that the CRISPR-Cas9 editing enhancement by Repsox observed here is attributed to the promotion of an error-prone alternative repair pathway that is distinct from classical NHEJ. As reported by Weaver et al.,[40] inhibition of TGF-β signaling leads to delay in recruitment of both NHEJ and HDR repair factors, raising the possibilities of the alternative pathway in repair of DSBs. Previous studies have shown the increase

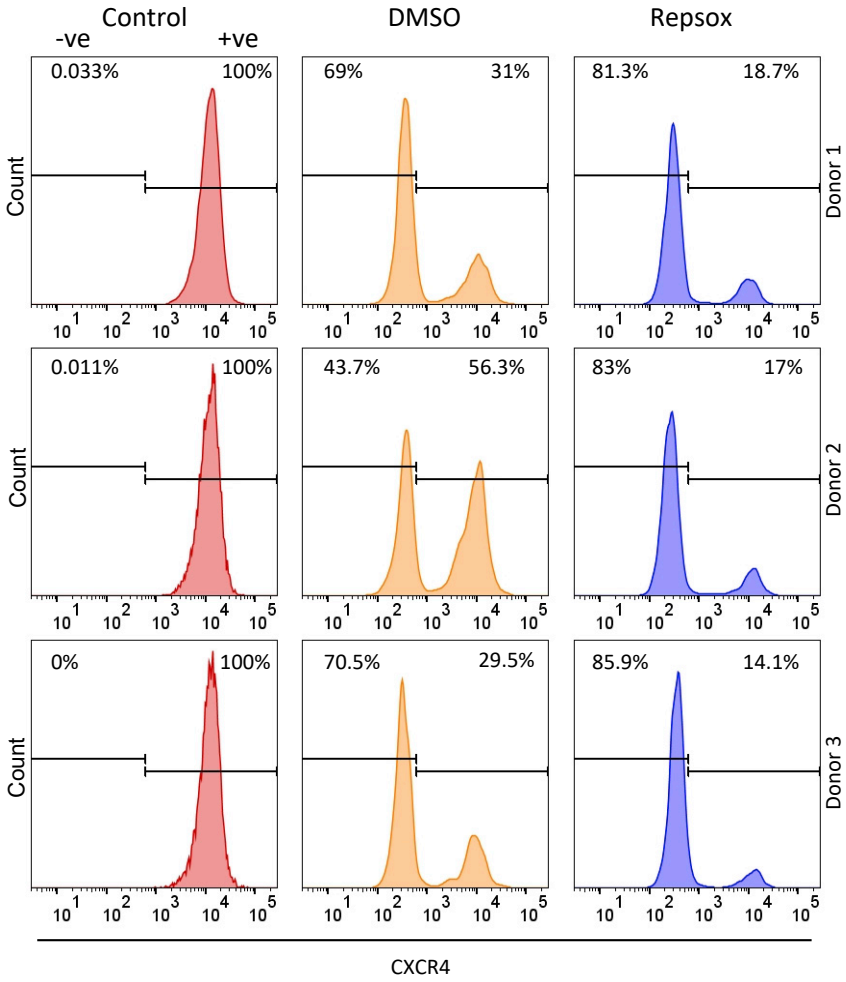

Figure 7. Repsox enhances editing in primary cells
Representative flow cytometry profiles indicate Repsox-enhanced loss of *CXCR4* expression in human primary $CD4^+$ T cells from three different donors.

of alternative NHEJ pathways in the absence of canonical NHEJ factors such as DNA LIG4 (a target of TGF-β). Another report[41] suggested that the inhibition of TGF-β signaling by small molecules leads to a reduction in HDR and c-NHEJ-based DSB repair but an increase in the alternative NHEJ. It appears that inhibition of TGF-βRI by Repsox treatment plausibly leads to the shift of DSB repair from c-NHEJ to a more error-prone alternative NHEJ pathway that results in an enhancement of loss-of-function editing.

Targeted genome editing using CRISPR-Cas9 introduces new prospects for generating cell-based disease models and treating life-threatening conditions. Although proven promising, the technical hurdles related to delivery and low efficiency in primary cells still presented a stiff challenge.[42,43] In contrast to HDR, which is active mainly during the S/G2 phase, NHEJ is active throughout the entire cell cycle and is therefore easier to harness for therapeutic genome engineering. For this reason, studies have focused on disrupting genes, for example, to produce HIV-resistant T cells and non-alloreactive CAR-T cells.[24,44] Particularly with suboptimal delivery conditions, our approach of combining small molecules for transiently blocking inhibitory signals in primary cells suggests a viable option for therapeutic genome editing. Our approach is also expected to facilitate the generation of infection-resistant cells as well as the CAR-T cell products.

In sum, temporary blocking of potentially competing signals by small molecules may practically be a useful adjunct to achieve higher genome editing. Moreover, it is conceivable to combine such small-molecule targeting approaches with CRISPR-Cas9 genome editing to deepen our understanding of the spatiotemporal dynamics of DSB repair mechanisms in various cell types.

MATERIALS AND METHODS

Cell culture and reagents

HeLa, HT1080, MCF7, and A549 were obtained from the American Type Culture Collection (ATCC). HEK293T (ECACC) and JurkatTAg (JTAg) were reported earlier in Rosa et al.[23] K562 and SW480 were obtained from National Centre for Cell Science (NCCS). HEK293T, HeLa, K562, HT1080, SW480, and A549 cells were cultured in DMEM (Gibco) supplemented with 10% fetal bovine serum (FBS; U.S. origin, certified, heat-inactivated serum; Gibco), 2 mM GlutaMAX, and 1× penicillin-streptomycin (Gibco). JTAg cells were grown in RPMI (Biowest) supplemented with 10% FBS, 2 mM GlutaMAX, and 1× penicillin-streptomycin. Cells were cultured in a humidified incubator at 37°C with 5% CO_2. All the chemicals were procured from Sigma-Aldrich unless otherwise specified.

Plasmids

For the rapid assessment of expression loss resulting from CRISPR-Cas9 targeting, we engineered mGFP plasmid with a cassette for modified GFP expression. The reduction in the half-life of the GFP was achieved by fusing it with a CDB nucleotide sequence, which was amplified from JTAg cDNA using forward GCCACCATGG CGCTCCGAGTCACCAG and reverse TCTTTAACAGGCTCAGG TTC primers. A lentiviral pScalps mGFP puro vector was constructed for generating stable cell lines for loss-of-function editing assays. For this, an mGFP encoding sequence was released from the parental mGFP plasmid with NheI/NotI and cloned into a lentiviral mammalian expression vector pScalps_Puro (a kind gift from Silvia Monticelli; plasmid 99636; Addgene) with XbaI/NotI sites. The

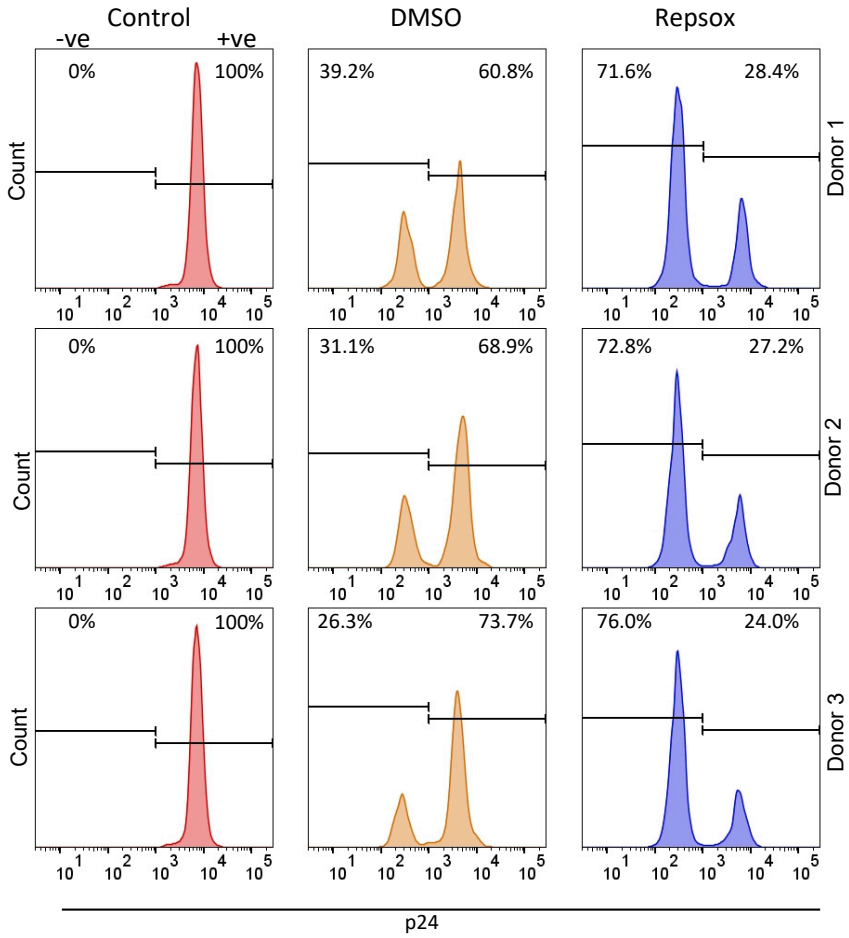

Figure 8. Generation of HIV-1-resistant CD4⁺ T cells by small molecule-assisted editing

CXCR4 loss-of-function editing and concomitant resistance of the CD4⁺ T cells to X4-tropic HIV-1 infection as assessed by HIV-1 capsid (p24) staining in the *CXCR4*-edited cells that received either DMSO or Repsox.

custom-designed vector for co-expression of Cas9 and Zsgreen, pScalps-eSpCas9-Zsgreen, was constructed from the parent pLenti-CRISPR-E (78852; Addgene) for eSpcas9 expression in cell lines and primary cells. pScalps-eSpcas9-Zsgreen plasmid was further modified to include a U6-driven gRNA expression cassette. The guide RNAs were cloned either at BsmBI or BbsI sites in pLentiCRISPR-E or pX458 or pScalps-eSpCas9-Zsgreen (48138; Addgene). To generate the vector expressing gRNA alone, the SpCas9-GFP cassette was removed from the pX458 plasmid by XbaI/NotI digestion, and the plasmid was self-ligated after end repair, resulting in the plasmid named pX458ΔCas9 gRNA scaffold. For editing the *SERINC5* locus in various cells, pX458ΔCas9 gRNA SERINC5 was generated by removing the SpCas9-GFP by XbaI/NotI and used with Cas9-expressing plasmid.

To develop $tRNA_{Gln}$-sgRNA (single guide RNA) expression construct, overlapping PCR was performed using oligonucleotides to generate tRNA fused to sgRNA. The amplified product was cloned in pTZ57R using HindIII and EcoRI.[45]

The plasmids and primers list are provided in Tables S1 and S2, respectively.

Generation of stable cell lines

To generate cells lines that stably express mGFP, HEK293T and JTAg cells were transduced with lentiviruses carrying mGFP reporter (multiplicity of infection [MOI] = 0.1). HEK293T and JTAg cells were sorted using FACS Aria (BD Biosciences) to generate a pure population expressing mGFP. The A549, HeLa, HEK293T, HT1080, K562, and JTAg luciferase cell lines were created using lentiviral infection (MOI = 0.1), and the transduced population was selected with puromycin (Invivogen).

Half-life determination of CDB-GFP

HEK293T cells (0.1×10^6) were seeded in a 24-well plate. At 50% confluency, cells were transfected (at $T = -12$ h) using the calcium phosphate method with pLentiCRISPR E (200 ng), pX458 gRNA GFP ΔCas9 (200 ng) (target gRNA)/pX458 gRNA FLucΔCas9 (control gRNA) (200 ng), and pCDB-GFP N1 (50 ng) pTAG-RFP657 (50 ng) (transfection control). RFP cell count, GFP cell count, and GFP intensity were monitored for $T =$ 0, 6, 12, 24, and 48 h using a SpectraMaxi3X multimode reader (Molecular Devices).

Small molecules

A library of 1,280 biologically active small molecules was procured from Tocris Bioscience. Repsox was procured from Tocris Bioscience and Sigma-Aldrich. Repsox was diluted in PBS to obtain 1–20 mM stock concentration.

The details of the compound and the sources are provided in the supplemental information (Table S3).

Characterization of compounds by LC-MS

Repsox was diluted in DMSO at a final concentration of 1 μg/mL for liquid chromatography-mass spectrometry (LC-MS) analysis (Nano-LC MALDI TOF/TOF spectrometer) using DMSO as a control. Peaks were analyzed for Repsox to validate the identity of the molecule.

Small-molecule screen and loss-of-function editing assay

The small-molecule screen for loss-of-function editing was performed as follows. HEK293T cells were seeded at 60%–70% confluency into a 10 cm^2 plate. Briefly, eSpCas9 (3 μg), pX458

gRNA GFP/gRNA FLuc ΔCas9 (3 μg), pCDB-GFP (500 ng), and pTAG-RFP657 (500 ng) were co-transfected using the calcium phosphate method. Post-transfection, the cells were trypsinized and reseeded with 5,000 cells per well in a 96-well plate. The small molecules were added to each well at 10 μM final concentration for 48 h. The cells were fixed using 4% paraformaldehyde (PFA) (F1635; Sigma Aldrich), washed three times with 1× PBS (SH30256.02; Hyclone), and resuspended in 1× PBS for imaging. The numbers of GFP- and RFP-positive cells were scored using a Spectramaxi3X Multimode imaging cytometer. The ratio of RFP/GFP was calculated for each molecule to appraise the editing efficiency. To overcome variation due to transfection efficiency and plate effect, no editing and DMSO controls were included in every plate, and the average RFP/GFP ratio was used to set the baseline of GFP editing.

For hit selection, a cut-off of GFP loss ($\geq$1.5 fold) was set for pre-selection of top hits in the primary screen. Eighty-two small molecules were selected for the secondary analysis. The secondary screen was performed in at least triplicate. Subsequently, the hits that continued to reproduce in these trials were then tested in different independent experiments with mGFP stable HEK293T cells.

The Z factor (Z′) for NHEJ primary and the secondary screen was calculated as follows:

$$Z' = 1 - 3(\sigma 1 + \sigma 2)/(\mathrm{I}\ \mu 1 - \mu 2 I),$$

where σ1 and σ2 are the SDs of control (eSpCas9+gRNA luciferase) and eSpCas9+gRNA GFP-transfected population, respectively, and μ1 and μ2 are the means of RFP/GFP ratio of control and eSpCas9+gRNA GFP transfected controls, respectively.

The raw data values of the screens are provided in the supplemental information (Table S3).

Sanger sequencing and TIDE analysis

To confirm that the loss of GFP was due to GFP locus editing, we isolated the genomic DNA of mGFP stable HEK293T cells, co-transfected with eSpcas9 and gRNA GFP/Fluc. Next, we amplified the GFP locus by PCR using (100 ng genomic DNA template) GFP locus-specific oligos. Both the control and edited locus were eluted from agarose gels, and Sanger sequencing was performed. The editing at the GFP locus was confirmed using TIDE analysis (https://tide.nki.nl).[46]

Luciferase assay

The luciferase assay was performed in 96-well plates. The cells were first lysed using 100 μL lysis buffer (1% Triton X-100, 25 mM tricine [pH 7.8], 15 mM potassium phosphate, 15 mM $MgSO_4$, 4 mM EGTA, and 1 mM DTT) for 20 min at room temperature, and luminescence readings were obtained using a Spectramaxi3X plate reader in injector mode, by mixing 50 μL cell lysate supernatant with 50 μL substrate buffer (lysis buffer with 1 mM ATP, 0.2 mM D-luciferin).[47]

Flow cytometry

For analysis by flow cytometry, HEK293T mGFP cells were seeded in 24-well plates 24 h before transfection (70% confluency) and co-transfected with Cas9 (200 ng), pX458ΔCas9 gRNA-GFP/Luc (200 ng) plasmids using the calcium phosphate method. After 8 h of transfection, cells were trypsinized and reseeded in 96-well plates (10,000 cells/well). DMSO and Repsox (10 μM) were added in respective wells. After 48 h of drug treatment, cells were trypsinized (25200056; Gibco), harvested, and finally resuspended in 1× PBS and fixed with 4% PFA for 20 min at room temperature. Fixed cells were washed three times with 1× PBS and taken for flow cytometry analysis. Similarly, suspension cells were collected, washed, and processed for flow cytometry. Sample acquisition was done using FACS Aria III (BD Biosciences), and the data were analyzed using FlowJo software (FlowJo).

For the analysis of *CXCR4* editing in JTAg cells, 1×10^7 cells were electroporated using Bio-Rad Gene PulserXcell with eSpCas9 (5 μg), px458 gCXCR4 ΔCas9/gFLuc ΔCas9 (5 μg). After electroporation, cells were split into different wells. DMSO and Repsox (10 μM) were added to the respective wells. After 72 h of electroporation, the cells were collected in microcentrifuge tubes and washed with 1× PBS. Following this, they were washed twice with 1 mL PBA (PBS, 1% BSA, 0.1% Na azide) and resuspended in 100 μL of staining solution (CXCR4 antibody 1:500) (NIH AIDS reagent program). After 1 h, cells were washed thrice with PBA and resuspended in 100 μL secondary staining solution (anti-mouse Alexa 633 1:1,000) (Thermo Fisher Scientific) for 1 h. The cells were then washed thrice with PBA and taken for fluorescence-activated cell sorting (FACS) analysis.

$CD4^+$ T cell isolation from blood

After consent from healthy donors, blood was collected in preservative-free anticoagulant (0.2% final concentration of EDTA) and processed immediately for peripheral blood mononuclear cell (PBMC) isolation. PBMC isolation was done with the help of Histopaque using the manufacturer's protocol (catalog no. 10771; Sigma-Aldrich). Precisely 3 mL blood was layered on the top of an equal amount of Histopaque-1077. Afterward, the sample was carefully centrifuged in a swing bucket rotor, keeping acceleration and brake at the lowest setting at 400 × *g* for 30 min at room temperature. Following centrifugation, cells from the opaque interface were transferred to a fresh centrifuge tube. Cells were washed twice with isotonic phosphate buffer saline collected upon centrifugation at 250 × *g* for 10 min. Finally, cells were resuspended in the isotonic phosphate buffer saline or RPMI-1640 (catalog no. L0500-500; Biowest) and processed further for the $CD4^+$ cell isolation.

$CD4^+$ T cells were isolated from fresh PBMCs by magnetic separation with a $CD4^+$ isolation kit (catalog no. 130-045-101; Miltenyi Biotec) as described in the manufacturer's protocol. Isolated $CD4^+$ T cells were characterized using FACS after counter-staining with anti-CD4-APC antibody (1:20 in PBA) (130-113-812 - CD4-APC, human; Miltenyi Biotec) and anti-CD3-FITC labeled antibody.

Primary CD4+ T cell maintenance and expansion

Primary $CD4^+$ T cells were grown and maintained in RPMI-1640 (Biowest). For $CD4^+$ T cell expansion, the medium was supplemented with 5 μg/mL PHA (Sigma-Aldrich) and 50 IU/mL recombinant human IL-2 (Gibco). IL-2 was also added to every culture at a 50 IU/mL final concentration. Cells were maintained in IL-2 containing medium for experimental purposes.

Vector production and CXCR4 editing in CD4+ primary T cells

For lentiviral vector production, pScalps eSpCas9 Zsgreen gCXCR4/gLuc (8 μg), psPAX2 (6 μg), and pMD2.g (2 μg) were co-transfected in HEK293T cells using the calcium phosphate method in a 10 cm^2 cell culture dish, seeded 1 day before transfection. After 12–15 h, the medium was replaced with the fresh medium, and cells were maintained for the next 48 h. After 48 h, the virus-containing supernatant was filtered and concentrated at 100,000 × *g* using a 20% sucrose (in 1× PBS) cushion by ultracentrifugation. $CD4^+$ cells were transduced at MOI = 5 with viruses in the presence of DMSO and Repsox. After 5 days of treatment, cells were collected and processed for FACS analysis. Briefly, for blocking, $CD4^+$ cells were resuspended in ice-cold PBA and incubated for 15 min. Next, cells were collected by centrifugation at 500 × *g* for 5 min and incubated on ice with a primary CXCR4 antibody (1:500 dilution in PBA) for 3 h. Post-incubation, cells were washed thrice using ice-cold PBS and further incubated with secondary antibody Alexa 633 (1:500) for 1 h. Finally, cells were washed with 1× PBS to remove unbound antibodies and analyzed by FACS.

HIV-1 virus production, CD4+ primary T cell infection, and p24 staining

To infect $CD4^+$ primary T cells, we generated HIV-1 particles using HEK293T as a virus producer cells by co-transfecting 7 μg pNL4-3 Env^-Nef^- and 1 μg pHXB2 X4-tropic envelope[48] in a 10 cm^2 cell culture dish using the calcium phosphate transfection method. The next morning, after 12–15 h, the medium was replaced with fresh medium, and cells were maintained for the next 48 h. Post-incubation, virus-containing supernatant was clarified using centrifugation at 300 × *g* for 5 min. The supernatant was filtered using a 0.22 μm syringe filter (Millipore). Next, the viral supernatant was overlaid on a 20% sucrose (in 1× PBS) cushion and concentrated at 100,000 × *g* for 2 h at 4°C using an ultracentrifuge. After the spin, the supernatant was aspirated, and the pellet was resuspended in 1× PBS. For primary cells infection (*CXCR4* edited pool), 80,000 $CD4^+$ T cells were seeded in 24-well formats. Furthermore, these cells were infected using X4-tropic HIV-1 at MOI = 5. Cells were maintained for 5 days. Following this, cells were collected and fixed using 2%–4% PFA and processed for FACS analysis. Cells were resuspended in BD Perm/Wash Buffer and incubated for 15 min. Next, cells were collected using centrifugation at 500 × *g* for 5 min and incubated on ice with 100 μL primary P24 antibody (NIH ARP; 1:500 dilution in Perm/Wash Buffer) for 3 h. Post-incubation, cells were washed thrice using 1× PBS and further incubated with 100 μL secondary antibody Alexa 633 (1:500) for 1 h. Finally, cells were washed with 1× PBS to remove unbound antibodies and analyzed using FACS.

Cell viability assay

HEK293T, HT1080, and A549 cells were seeded in 96-well plates (10,000/well) and co-transfected with plasmids encoding Cas9 (50 ng) and guide RNA (50 ng) using Lipofectamine 3000. Cells were treated with Repsox at different concentrations (0.1, 0.5, 1, 5, 10, 20, and 50 μM) for 48 h. After 48 h of compound addition, Alamar Blue reagent (HiMedia) was added to each well according to the manufacturer's protocol, and the plate was incubated at 37°C for 4 h. The absorbance was measured at 570 nm using a SpectraMaxi3X plate reader.

SMAD inhibition reporter assay

To check the effect of Repsox on the inhibition of the TGF-βRI pathway, we used the SMAD reporter plasmid SBE4-Luc (16495; Addgene). This plasmid contains the luciferase reporter gene under the SMAD binding elements, which expresses under the influence of TGF-βRI-mediated signaling. To check the effect of Repsox on loss-of-function editing enhancement, HEK293T mGFP cells were seeded in a 24-well plate 24 h before transfection. Next, cells were transfected with SBE4-Luc, pRL-TK, along with Cas9 and gGFP/gRFP plasmids. The transfected cells were treated with Repsox for the next 48 h. The magnitude of GFP loss was estimated by GFP cell count and normalized to total cell count. Luciferase activity was measured by luciferase assay. The luciferase units were normalized with Renilla luciferase units.

Cas9 VLPs production and target cells transduction

To produce virus-like particles carrying Cas9 and guide RNA, HEK293T cells were seeded in a 10 cm^2 plate and co-transfected with pcDNA-Cas9 (10 μg), pTZ tRNA (glutamine) gGFP/gFluc (10 μg), and pMD2.G (10 μg) using the calcium phosphate method. The medium was replaced with a fresh medium after 12–16 h of transfection. The Cas9 VLP-containing medium was collected after 48 h of transfection and filtered using a 0.22 μm filter to remove cell debris. Cas9 VLPs were concentrated by ultracentrifugation at 100,000 × *g* for 2 h at 4°C. Concentrated VLPs were resuspended in a cell culture medium. The target cells were seeded 1 day before transduction and were challenged with VLPs by spinoculation at 1,200 × *g* for 1 h.

Western blotting

For western blotting, samples were prepared in a 4× Laemmli buffer and run on either 8% or 12% Tris-tricine gels for electrophoresis depending upon the molecular weight range being detected using this method. Following this, gels were electro-blotted on the polyvinylidene fluoride (PVDF) membrane (Immobilon-FL; Merck-Millipore). Blocking of membranes was carried out by incubation with the Odyssey Blocking Buffer (LI-COR Biosciences) for 20–30 min, followed by both primary and secondary antibody incubations for 1 h each at room temperature, each of which was followed by three washes of 5 min each.

Detection of Cas9 and β-actin was carried out using mouse anti-Cas9 antibody (Clontech) and rabbit anti-beta actin antibody (LI-COR Biosciences), respectively. Secondary antibodies used were either IR dye 680 goat anti-mouse or IR dye 800 goat anti-rabbit (LI-COR Biosciences).

For immunoblotting of proteins incorporated into virus-like particles, the particle-containing supernatant was concentrated on a sucrose cushion by ultracentrifugation at 100,000 × *g* for 2 h at 4°C. The pellet obtained was resuspended in the 2× Laemmli buffer containing 2X-PIC (protease inhibitor cocktail) and 50 mM TCEP (Tris[2-carboxyethyl]phosphine hydrochloride).

Neutral comet assay

A modified neutral comet assay procedure was followed as previously described.[49] HEK293T cells were trypsinized after 48 h Repsox treatment and resuspended at 4 × 10^4 cells/mL in 1× PBS. Cells were mixed with low melting agarose (1%) (VWR Life Science) at a 1:5 ratio and spread over the slide pre-coated with normal agarose. Slides were dried at room temperature for 2–5 min and immersed into neutral lysis buffer (2.5 M NaCl, 0.1 M EDTA, 10 mM Trizma base [pH 10], 1% N-laurylsarcosine, 0.5% Triton X-100, and 10% DMSO) overnight at 4°C. The next day the slides were immersed into pre-chilled neutral electrophoresis buffer (300 mM sodium acetate, 100 mM Tris-HCl [pH 8.3]) for 30 min, followed by electrophoresis for 45 min at 4°C. Subsequently, the slides were incubated in DNA precipitation solution (DPS) for 30 min at room temperature, followed by 30 min incubation in 70% ethanol. Slides were dried for 2 h at room temperature and stained with EtBr solution (2 μg/mL in water). Images were acquired using a Zeiss Apotome fluorescence microscope (Carl Zeiss) using a 10× objective lens, and the tail moments were quantified using the OpenComet (https://cometbio.org/). For each condition, at least 50 cells were analyzed using OpenComet.[50]

Next-generation sequencing

To analyze the occurrence of indels in off-target genes, genomic DNA was extracted from Repsox-treated *CXCR4*-edited cells (HEK293T and JTAg). A 200 bp nucleotide fragment was amplified by PCR using an adapter containing specific primers (Table S2). A subsequent limited-cycle amplification step was performed to add multiplexing indices and Illumina sequencing adapters. Normalized and pooled libraries were then sequenced on the Illumina MiSeq system using v3 reagents (2 × 300 nt paired-end reads). For the off-target editing analysis, CRISPResso2 was used to process fastq.gz files obtained from the Illumina sequencing run.[51] Reads were mapped to the predicted amplicon, and mutation frequencies were quantified using a computational pipeline.

The "-min_average_read_quality" flag was set to 30 to filter out reads with average phred33 quality scores less than 30. The data are available as Bio project #PRJNA793002.

Effect of Repsox on Cas9 expression

To check the effect of Repsox on Cas9 expression, HEK293T (0.3 × 10^6) cells were seeded in a 35 mm plate and transfected with 1 μg Cas9-expressing plasmid. Furthermore, the cells were treated with DMSO or Repsox (5 and 10 μM) for the next 48 h. Following this, the cells were collected in cold PBS and lysed using RIPA buffer supplemented with a 2× protease inhibitor cocktail and 50 mM TCEP. Cell lysate was collected after removing cell debris and mixed with 4× Laemmli buffer and run on 8% Tris-tricine gel followed by Cas9 detection as described above.

EdU incorporation assay

To measure the effect of Repsox treatment on cell cycle, HEK293T, K562, and JTAg cells were seeded in a 35 mm plate at a density of 0.1 × 10^6 and cultured for the next 48 h in the presence of DMSO/Repsox. EdU (10 μM) (Sigma-Aldrich) was added 6 h before collection of cells. Subsequently, cells were washed thrice with PBS and fixed using 4% paraformaldehyde. Furthermore, the cells were permeabilized with 0.05% Triton X-100 for 5 min and washed twice with 1× PBS. Next, the cells were incubated for 30 min with 5 μM sulfo-cy5 azide (from stock 10 mM), 0.1 M Tris-Cl (from 1 M stock [pH 8.5]), 4 mM $CuSO_4$ (from 1 M stock), and 100 mM sodium ascorbate (0.5 M stock).[52] Cells were washed thrice with 1× PBS after staining. The staining solution was prepared fresh each time before use. After staining, cells were taken for analysis by FACS.

TGF-βRI-knockout cell generation and western blot

For the generation of TGF-βRI-knockout cells, HEK293T and HeLa cells were transduced with lentiviral vectors carrying guide RNA against TGF-βRI in the presence of Repsox (10 μM). Furthermore, transduced cells were selected for 2 weeks with 1 μg/mL puromycin. To confirm TGF-βRI knockout, cells were collected in ice-cold 1× PBS using scrapper and lysed with RIPA lysis buffer (supplemented with 2X-PIC and 50 mM TCEP). Cell debris was removed before collecting cell lysate. Furthermore, cell lysate was mixed with 4× Laemmli buffer and run on 12% Tris-tricine gel. Following this, proteins were electro-blotted on the PVDF membrane (Immobilon-FL). Blocking of the membrane was carried out by incubation with the Blocking Buffer (Bio-Rad) for 30 min at room temperature, followed by both primary (AF3025-SP Human TGF-βRI/ALK5 Antibody; Novusbio) and secondary antibody (IRDYe 680 Donkey anti-Goat; Thermo Fisher Scientific) incubations for 1 h each at room temperature, each of which was followed by three washes of 5 min each. Actin served as the loading control in the western blot.

Fold change analysis

The following formula was used to calculate the gene-editing fold enhancement:

$$Fold\ Change\ = \frac{Percentage\ of\ gLuc - percentage\ of\ gGFP\ (Repsox)or\ gCXCR4}{(percentage\ of\ gLuc - percentage\ of\ gGFP(DMSO))}.$$

Software and statistical analysis

The significance of results was statistically analyzed using Student's unpaired t test using GraphPad Prism 9. The relative differences were considered statistically significant at $p < 0.05$. The significance in the results is denoted as follows: *$p < 0.05$, **$p < 0.01$, ***$p < 0.001$, and ****$p < 0.0001$; and ns, not significant. Specific portions of images were produced using BioRender.

Data reporting

No statistical methods were used to predetermine sample size. Investigators were blinded to the allocation of small molecules during experiments and outcome assessment for checking the robustness and reproducibility of the phenotypes. Investigators were not blinded in any other experiments or outcome assessments. The deep sequencing data generated in this study are uploaded to the National Center for Biotechnology Information (NCBI) and can be accessed with ID Bio project #PRJNA793002.

Ethics statement

The study involving peripheral blood cells from healthy donors was approved by the institutional ethics committee.

SUPPLEMENTAL INFORMATION

Supplemental information can be found online at https://doi.org/10.1016/j.omtn.2022.03.003.

ACKNOWLEDGMENTS

This work was supported by grants from the Department of Biotechnology (DBT) (grant BT/PR26013/GET/119/191/2017) and the Wellcome Trust/DBT India Alliance (IA/I/18/2/504006 awarded to A.C.). T.M. and P.R. are supported by a fellowship from the MHRD. V.B. and N.A. are supported by a CSIR fellowship. The authors are thankful to Massimo Pizzato and the NIH AIDS reagent program for the reagents and cell lines.

AUTHOR CONTRIBUTIONS

Methodology, T.M., V.B., N.A., P.G., P.R., S.S., and A.C.; Investigation, T.M., V.B., N.A., S.S., and A.C.; Visualization, T.M., V.B., S.S., and A.C.; Conceptualization, A.C.; Supervision, A.C.; Writing – Original Draft, T.M. and A.C.; Writing – Review & Editing, T.M., V.B., N.A., P.R., P.G., S.S., and A.C.

DECLARATION OF INTERESTS

The authors declare no competing interests.

REFERENCES

1. Doudna, J.A., and Charpentier, E. (2014). The new frontier of genome engineering with CRISPR-Cas9. Science *346*, 1258096.
2. Peng, R., Lin, G., and Li, J. (2016). Potential pitfalls of CRISPR/Cas9-mediated genome editing. FEBS J. *283*, 1218–1231.
3. Pulecio, J., Verma, N., Mejía-Ramírez, E., Huangfu, D., and Raya, A. (2017). CRISPR/Cas9-Based engineering of the epigenome. Cell Stem Cell *21*, 431–447.
4. Vasquez, J.J., Wedel, C., Cosentino, R.O., and Siegel, T.N. (2018). Exploiting CRISPR-Cas9 technology to investigate individual histone modifications. Nucleic Acids Res. *46*, E106.
5. Lackner, D.H., Carré, A., Guzzardo, P.M., Banning, C., Mangena, R., Henley, T., Oberndorfer, S., Gapp, B.V., Nijman, S.M.B., Brummelkamp, T.R., et al. (2015). A generic strategy for CRISPR-Cas9-mediated gene tagging. Nat. Commun. *6*, 1–7.
6. Schwinn, M.K., Machleidt, T., Zimmerman, K., Eggers, C.T., Dixon, A.S., Hurst, R., Hall, M.P., Encell, L.P., Binkowski, B.F., and Wood, K.V. (2018). CRISPR-mediated tagging of endogenous proteins with a luminescent peptide. ACS Chem. Biol. *13*, 467–474.
7. Wang, H., Nakamura, M., Abbott, T.R., Zhao, D., Luo, K., Yu, C., Nguyen, C.M., Lo, A., Daley, T.P., La Russa, M., et al. (2019). CRISPR-mediated live imaging of genome editing and transcription. Science *365*, 1301–1305.
8. Frangoul, H., Altshuler, D., Cappellini, M.D., Chen, Y.-S., Domm, J., Eustace, B.K., Foell, J., de la Fuente, J., Grupp, S., Handgretinger, R., et al. (2021). CRISPR-Cas9 gene editing for Sickle cell disease and β-Thalassemia. N. Engl. J. Med. *384*, 252–260.
9. Kanaar, R., Hoeijmakers, J.H.J., and Van Gent, D.C. (1998). Molecular mechanisms of DNA double-strand break repair. Trends Cell Biol. *8*, 483–489.
10. Wu, W.Y., Lebbink, J.H.G., Kanaar, R., Geijsen, N., and Van Der Oost, J. (2018). Genome editing by natural and engineered CRISPR-associated nucleases. Nat. Chem. Biol. *14*, 642–651.
11. Chapman, J.R., Taylor, M.R.G., and Boulton, S.J. (2012). Playing the end game: DNA double-strand break repair pathway choice. Mol. Cell *47*, 497–510.
12. Ichida, J.K., Blanchard, J., Lam, K., Son, E.Y., Chung, J.E., Egli, D., Loh, K.M., Carter, A.C., Di Giorgio, F.P., Koszka, K., et al. (2009). A small-molecule inhibitor of Tgf-β signaling replaces Sox2 in reprogramming by inducing Nanog. Cell Stem Cell *5*, 491–503.
13. Tu, W. zhi, Fu, Y. bin, and Xie, X. (2019). RepSox, a small molecule inhibitor of the TGFβ receptor, induces brown adipogenesis and browning of white adipocytes. Acta Pharmacol. Sin. *40*, 1523–1531.
14. Massagué, J. (2012). TGFβ signalling in context. Nat. Rev. Mol. Cell Biol. *13*, 616–630.
15. Lee, J., Kim, M.R., Kim, H.J., An, Y.S., and Yi, J.Y. (2016). TGF-β1 accelerates the DNA damage response in epithelial cells via Smad signaling. Biochem. Biophys. Res. Commun. *476*, 420–442.
16. Liu, Q., Ma, L., Jones, T., Palomero, L., Pujana, M.A., Martinez-Ruiz, H., Ha, P.K., Murnane, J., Cuartas, I., Seoane, J., et al. (2018). Subjugation of TGFβ signaling by human papilloma virus in head and neck squamous cell carcinoma shifts DNA repair from homologous recombination to alternative end joining. Clin. Cancer Res. *24*, 6001–6014.
17. Corish, P., and Tyler-Smith, C. (1999). Attenuation of green fluorescent protein half-life in mammalian cells. Protein Eng. *12*, 1035–1040.
18. Blokpoel, M.C.J., O'Toole, R., Smeulders, M.J., and Williams, H.D. (2003). Development and application of unstable GFP variants to kinetic studies of mycobacterial gene expression. J. Microbiol. Methods *54*, 203–211.
19. Andersen, J.B., Sternberg, C., Poulsen, L.K., Bjørn, S.P., Givskov, M., and Molin, S. (1998). New unstable variants of green fluorescent protein for studies of transient gene expression in bacteria. Appl. Environ. Microbiol. *64*, 2240.
20. Glotzer, M., Murray, A.W., and Kirschner, M.W. (1991). Cyclin is degraded by the ubiquitin pathway. Nature *349*, 132–138.
21. Slaymaker, I.M., Gao, L., Zetsche, B., Scott, D.A., Yan, W.X., and Zhang, F. (2016). Rationally engineered Cas9 nucleases with improved specificity. Science *351*, 84–88.
22. Yu, C., Liu, Y., Ma, T., Liu, K., Xu, S., Zhang, Y., Liu, H., La Russa, M., Xie, M., Ding, S., et al. (2015). Small molecules enhance CRISPR genome editing in pluripotent stem cells. Cell Stem Cell *16*, 142–147.
23. Rosa, A., Chande, A., Ziglio, S., De Sanctis, V., Bertorelli, R., Goh, S.L., McCauley, S.M., Nowosielska, A., Antonarakis, S.E., Luban, J., et al. (2015). HIV-1 Nef promotes infection by excluding SERINC5 from virion incorporation. Nature *526*, 212–217.
24. Hou, P., Chen, S., Wang, S., Yu, X., Chen, Y., Jiang, M., Zhuang, K., Ho, W., Hou, W., Huang, J., et al. (2015). Genome editing of CXCR4 by CRISPR/cas9 confers cells resistant to HIV-1 infection. Sci. Rep. *5*, 1–12.
25. Matsumoto, D., Tamamura, H., and Nomura, W. (2020). A cell cycle-dependent CRISPR-Cas9 activation system based on an anti-CRISPR protein shows improved genome editing accuracy. Commun. Biol. *31*, 1–10.
26. Lu, Y., Liu, Y., and Yang, C. (2017). Evaluating in vitro DNA damage using comet assay. J. Vis. Exp. *2017*, 56450.
27. Ahuja, N., Ashok, C., Natua, S., Pant, D., Cherian, A., Pandkar, M.R., Yadav, P., Narayanan, S.S.,V., Mishra, J., Samaiya, A., et al. (2020). Hypoxia-induced TGF-β–RBFOX2–ESRP1 axis regulates human MENA alternative splicing and promotes EMT in breast cancer. NAR Cancer *2*, zcaa021.
28. Yeh, C.D., Richardson, C.D., and Corn, J.E. (2019). Advances in genome editing through control of DNA repair pathways. Nat. Cell Biol. *21*, 1468–1478.

29. Ray, U., and Raghavan, S.C. (2020). Modulation of DNA double-strand break repair as a strategy to improve precise genome editing. Oncogene *39*, 6393–6405.

30. Doudna, J.A. (2020). The promise and challenge of therapeutic genome editing. Nature *578*, 229–236.

31. Jajosky, A.N., Coad, J.E., Vos, J.A., Martin, K.H., Senft, J.R., Wenger, S.L., and Gibson, L.F. (2014). RepSox Slows Decay of CD34 + acute myeloid Leukemia cells and decreases T cell immunoglobulin mucin-3 expression. Stem Cells Transl. Med. *3*, 836–848.

32. Minami, I., Yamada, K., Otsuji, T.G., Yamamoto, T., Shen, Y., Otsuka, S., Kadota, S., Morone, N., Barve, M., Asai, Y., et al. (2012). A small molecule that promotes cardiac Differentiation of human pluripotent stem cells under Defined, cytokine- and Xeno-free conditions. Cell Rep. *2*, 1448–1460.

33. Kim, S., Kim, D., Cho, S.W., Kim, J., and Kim, J.S. (2014). Highly efficient RNA-guided genome editing in human cells via delivery of purified Cas9 ribonucleoproteins. Genome Res. *24*, 1012–1019.

34. Gaj, T., Staahl, B.T., Rodrigues, G.M.C., Limsirichai, P., Ekman, F.K., Doudna, J.A., and Schaffer, D.V. (2017). Targeted gene knock-in by homology-directed genome editing using Cas9 ribonucleoprotein and AAV donor delivery. Nucleic Acids Res. *45*, 98.

35. Zheng, H., Jarvis, I.W.H., Bottai, M., Dreij, K., and Stenius, U. (2019). TGF beta promotes repair of bulky DNA damage through increased ERCC1/XPF and ERCC1/XPA interaction. Carcinogenesis *40*, 580–591.

36. Liu, L., Zhou, W., Cheng, C.T., Ren, X., Somlo, G., Fong, M.Y., Chin, A.R., Li, H., Yu, Y., Xu, Y., et al. (2014). TGFβ Induces "bRCAness" and Sensitivity to PARP inhibition in breast cancer by regulating DNA-Repair Genes. Mol. Cancer Res. *12*, 1597–1609.

37. Zhang, H., Kozono, D.E., O'Connor, K.W., Vidal-Cardenas, S., Rousseau, A., Hamilton, A., Moreau, L., Gaudiano, E.F., Greenberger, J., Bagby, G., et al. (2016). TGF-β inhibition rescues hematopoietic stem cell defects and bone marrow failure in Fanconi anemia. Cell Stem Cell *18*, 668–681.

38. Kim, M.R., Lee, J., An, Y.S., Jin, Y.B., Park, I.C., Chung, E., Shin, I., Barcellos-Hoff, M.H., and Yi, J.Y. (2015). TGFβ1 protects cells from γ-IR by enhancing the activity of the NHEJ repair pathway. Mol. Cancer Res. *13*, 319–329.

39. Liu, S., Ren, J., and ten Dijke, P. (2021). Targeting TGFβ signal transduction for cancer therapy. Signal Transduct. Target. Ther. *6*, 1–20.

40. Weaver, A.N., Cooper, T.S., Rodriguez, M., Trummell, H.Q., Bonner, J.A., Rosenthal, E.L., and Yang, E.S. DNA double strand break repair defect and sensitivity to poly ADP-ribose polymerase (PARP) inhibition in human papillomavirus 16-positive head and neck squamous cell carcinoma. Oncotarget 6.26995-27007

41. Le, B.V., Podszywalow-Bartnicka, P., Maifrede, S., Sullivan-Reed, K., Nieborowska-Skorska, M., Golovine, K., Yao, J.C., Nejati, R., Cai, K.Q., Caruso, L.B., et al. (2020). TGFβR-SMAD3 signaling induces resistance to PARP inhibitors in the bone marrow microenvironment. Cell Rep. *33*, 108221.

42. Knopp, Y., Geis, F.K., Heckl, D., Horn, S., Neumann, T., Kuehle, J., Meyer, J., Fehse, B., Baum, C., Morgan, M., et al. (2018). Transient retrovirus-based CRISPR/Cas9 all-in-one particles for efficient, targeted gene knockout. Mol. Ther. - Nucleic Acids *13*, 256–274.

43. Montagna, C., Petris, G., Casini, A., Maule, G., Franceschini, G.M., Zanella, I., Conti, L., Arnoldi, F., Burrone, O.R., Zentilin, L., et al. (2018). VSV-G-Enveloped vesicles for traceless delivery of CRISPR-cas9. Mol. Ther. - Nucleic Acids *12*, 453–462.

44. Rafiq, S., Hackett, C.S., and Brentjens, R.J. (2020). Engineering strategies to overcome the current roadblocks in CAR T cell therapy. Nat. Rev. Clin. Oncol. *17*, 147–167.

45. Mefferd, A.L., Kornepati, A.V.R., Bogerd, H.P., Kennedy, E.M., and Cullen, B.R. (2015). Expression of CRISPR/Cas single guide RNAs using small tRNA promoters. RNA *21*, 1683–1689.

46. Brinkman, E.K., Chen, T., Amendola, M., and Van Steensel, B. (2014). Easy quantitative assessment of genome editing by sequence trace decomposition. Nucleic Acids Res. *42*, e168.

47. Mishra, T., Sreepadmanabh, M., Ramdas, P., Sahu, A.K., Kumar, A., and Chande, A. (2021). SARS CoV-2 Nucleoprotein enhances the infectivity of lentiviral spike particles. Front. Cell. Infect. Microbiol. *11*, 341.

48. Ramdas, P., Bhardwaj, V., Singh, A., Vijay, N., and Chande, A. (2021). Coelacanth SERINC2 inhibits HIV-1 infectivity and is counteracted by envelope glycoprotein from Foamy virus. J. Virol. *95*, e0022921.

49. Courilleau, C., Chailleux, C., Jauneau, A., Grima, F., Briois, S., Boutet-Robinet, E., Boudsocq, F., Trouche, D., and Canitrot, Y. (2012). The chromatin remodeler p400 ATPase facilitates Rad51-mediated repair of DNA double-strand breaks. J. Cell Biol. *199*, 1067.

50. Gyori, B.M., Venkatachalam, G., Thiagarajan, P.S., Hsu, D., and Clement, M.V. (2014). OpenComet: an automated tool for comet assay image analysis. Redox Biol. *2*, 457.

51. Clement, K., Rees, H., Canver, M.C., Gehrke, J.M., Farouni, R., Hsu, J.Y., Cole, M.A., Liu, D.R., Joung, J.K., Bauer, D.E., et al. (2019). Accurate and rapid analysis of genome editing data from nucleases and base editors with CRISPResso2. Nat. Biotechnol. *37*, 224.

52. Salic, A., and Mitchison, T.J. (2008). A chemical method for fast and sensitive detection of DNA synthesis in vivo. Proc. Natl. Acad. Sci. *105*, 2415–2420.